Astron. Astrophys. 347, 478–493 (1999)

ASTRONOMY AND ASTROPHYSICS

IUE observations of the high-velocity symbiotic star AG Draconis⋆

III. A compendium of 17 years of UV monitoring, and comparison with optical and X-ray observations

R. González-Riestra[1], **R. Viotti**[2], **T. Iijima**[3], **and J. Greiner**[4]

[1] Laboratorio de Astrofísica Espacial y Física Fundamental, VILSPA, P.O. Box 50727, E-28080 Madrid, Spain (ch@laeff.esa.es)
[2] Istituto di Astrofisica Spaziale, CNR, Area di Ricerca Tor Vergata, Via del Fosso del Cavaliere, I-00133 Roma, Italy (uvspace@saturn.ias.rm.cnr.it)
[3] Astronomical Observatory of Padova, Asiago Section, Osservatorio Astrofisico, I-36012 Asiago, Italy (iijima@astras.pd.astro.it)
[4] Astrophysical Institute Potsdam, An der Sternwarte 16, D-14482 Potsdam, Germany (jgreiner@aip.de)

Received 8 April 1999 / Accepted 29 April 1999

Abstract. We present the first extensive analysis of the ultraviolet observations with the IUE mission of the high velocity symbiotic system AG Draconis, covering the period June 1979–February 1996 which included three active phases of the system with six light maxima. The low resolution IUE line and continuum fluxes are compared with optical observations and with archival X-ray data. The analysis of the IUE observations near minimum (quiescence) led us to find that during the orbital motion the hot WD component is not eclipsed, in agreement with a non large inclination of the binary orbit. The larger modulation of the N V, C IV, He II, and O I lines with respect to the intercombination lines may indicate that the former are formed in a region near the line connecting the two stars, probably slightly receding, while the latter lines originate in an extended ionized nebula surrounding the white dwarf. Large orbit–to–orbit variation are probably associated with fluctuation of the K–star wind density. From the He II line we determine for the WD during quiescence a Zanstra temperature of 109600±5400°K, implying, at a distance of 2.5 kpc, a radius of 0.08±0.01 $R_{\odot}$, and a luminosity of 900±200 $L_{\odot}$.

During the different outbursts AG Dra displayed a variety of behaviours. According to the strength of the He II/FUV continuum ratio we have identified *cool* and *hot* outbursts. In fact, during the "minor" 1985–1986 outbursts the peak fluxes of the high ionization emission lines was comparable with those during the 1980–83 and 1994–95 major outbursts. The white dwarf temperature *decreased* to about 90000°K during the "cool" outbursts, while it *increased* to 120000–130000°K during the 1985–86 "hot" outbursts.

The behaviour during the major ("cool") outbursts is explained by expansion and cooling of the white dwarf atmosphere, which explains the marked *anticorrelation* between optical/UV and X–ray fluxes. The minimum X–ray flux observed also during the minor ("hot") outbursts might be attributed to the increased opacity of the WD envelope and wind to photons shortward the N^{+4} ionization limit. We also note that the beginning of the last activity phase of AG Dra was marked by the temporary appearance in July 1994 of strong P Cygni absorptions in the high ionization resonance lines with quite high terminal velocities of at least 700 km s^{-1}.

Key words: stars: binaries: symbiotic – stars: individual: AG Dra – stars: Population II – stars: white dwarfs – ultraviolet: stars – X-rays: stars

1. Introduction

The high–velocity, high–galactic latitude object AG Dra (BD+67°922) is the brightest symbiotic system in the ultraviolet which made it a good target for the IUE experiment. In addition, during the lifetime of IUE AG Dra underwent six light maxima (*outbursts*) in the visual which have been a unique opportunity for monitoring in the ultraviolet many outbursts of the same object. The IUE observations of AG Dra started in June 1979 and continued until January 1996, and have therefore covered a very long period of the stellar activity. Because of the largely varied activity of this object during this period, the IUE database is representing at the moment the unique and best way to study the activity of this interacting variable.

AG Dra is also known for being the most intense X–ray source among symbiotic stars (Anderson et al. 1981), and one of the best representatives of the category of the supersoft X–ray objects (Greiner 1996). Since the early HEAO-2 detection (Anderson et al. 1981), the star has been also observed with EXOSAT and ROSAT satellites. Actually, it was good luck that

Send offprint requests to: R. González-Riestra

⋆ Based on observations made with the International Ultraviolet Explorer collected at the Villafranca Satellite Tracking Station and retrieved from the IUE-INES Archive, on ROSAT observations, and on optical observations collected at the Asiago Observatory of the Padova Astronomical Observatory.

Correspondence to: R. González-Riestra

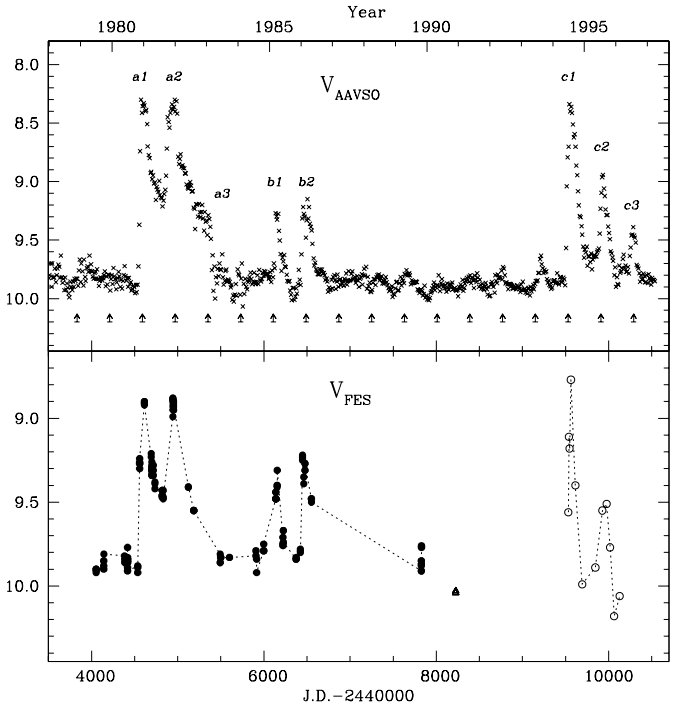

Fig. 1. *Upper panel:* Recent visual light curve of AG Dra based on the AAVSO observations (10–day means, Mattei 1997). The arrows indicate the predicted U-band light maxima according to the ephemeris given in Mikolajewska et al. (1995). *Lower panel:* IUE Fine Error Sensor (FES) light curve of AG Dra compiled along the 17 years of observations. The different symbols represent measurements taken at different positions in the FES camera: Filled circles: old Reference Point; triangles: new Reference Point; open circles: offset Reference Point (see text for details).

AG Dra underwent two minor outbursts (in 1985 and 1986) just during the lifetime of EXOSAT, which gave us the opportunity of observing for the first time the outburst of a symbiotic star in X–rays (Viotti et al. 1995). More recently, the ROSAT satellite monitored AG Dra during a long period of quiescence (1990–1993), and followed in greater detail the 1994 and 1995 outbursts (Greiner et al. 1997). ROSAT observations have been performed until 1998, and will hopefully give more interesting results on this X–ray symbiotic object. AG Dra was also observed by the HIPPARCOS satellite which has provided a lower limit of about 1 kpc to its distance, in agreement for a luminosity of the K star probably larger than that of a normal K–giant star (Viotti et al. 1997). It was also found that the astrometric position of AG Dra is coincident with the barycentre of the main radio source observed by Torbett & Campbell (1987), within the uncertainty of the radio observations.

In the previous papers we have analyzed the ultraviolet spectrum of AG Dra during its first major outburst (Viotti et al. 1983, Paper I), and have investigated the UV variation for the period from 1979 to 1983 which brackets the 1980–1983 active phase (Viotti et al. 1984, Paper II). More recently, we have studied the ultraviolet (IUE) and X–ray (ROSAT) emission of AG Dra during the 1994 and 1995 outbursts and during the previous quiescent phase (Greiner et al. 1997). We found that the hot component of the system is a white dwarf, which during its quiescent phase is burning hydrogen–rich matter on its surface at a rate of $3.2\times10^{-8}\ M_\odot\ \mathrm{y}^{-1}$ (for a distance of 2.5 kpc), which provides a luminosity of about 2500 $L_\odot$ and a surface temperature of 85000°K. The high accretion rate might be provided by a Roche lobe filling cool companion, though other mechanisms can be considered. The remarkable decrease of the X-ray flux during the 1994–95 optical maxima is very likely due to a temperature decrease of the hot component, as the result of a mass transfer increase causing an expansion of the compact star to about twice its original size. Extensive studies of the IUE observations of AG Dra have also been made among others, by Lutz et al. (1987), Kafatos et al. (1993) and Mikolajewska et al. (1995).

In this paper we make the first complete analysis of the full set of IUE low resolution images of AG Dra collected between June 1979 and February 1996. In addition, IUE data are complemented by optical spectrophotometry made at the Asiago Astrophysical Observatory during 1985–86 and 1993–97, and compared with the results of the X–ray observations with EXOSAT (1985–86) and ROSAT (1990–97) satellites. We finally discuss the results in the light of the interacting binary model of AG Dra.

2. AG Dra as a variable star

The light history of AG Dra can be traced back to the end of the nineteenth century (Robinson 1969). Photometrically, AG Dra is a variable which is normally at minimum (*quiescent phases*, Viotti 1993) with $\mathrm{m}_{pg}\ \sim\ 11$, V∼9.8–10.0 (Robinson 1969, Mattei 1997). AG Dra erratically undergoes 1–2 mag light maxima at time intervals from one to many years. Here, following Viotti (1993), we shall call *active phases* those periods of time between quiescent phases when AG Dra is significantly brighter than at minimum. These active phases are characterized by one or more light maxima which are commonly called *outbursts*, though this term might be not appropriate before knowing the physical nature of the light variations. The recent visual light curve of AG Dra, based on a slight smoothing of the 10–day mean light curve of the AAVSO database (Mattei 1997), is shown in Fig. 1. Though the curve is based on visual estimates from many different observers, nevertheless it represents the most complete quantitative description of the light history of AG Dra over the last twenty years. In the following we shall use the V value derived from this curve as the reference observational parameter which marks the *activity state* of AG Dra. When required, the V magnitudes are transformed into fluxes, assuming $\mathrm{F_V}$=$3.92\times10^{-9}10^{-0.4\mathrm{V}}$ erg cm^{-2} s^{-1} Å^{-1}. The AAVSO 10–day mean curve will also be used to determine the dates and time scales of the individual outbursts.

After a long period of quiescence (from 1969 to 1980) the star started by the end of 1980 a new *major* active phase characterized by two light maxima in November 1980 and in August 1981 (a_1 and a_2 in Fig. 1, see also Viotti et al. 1996) separated by about 360 days. A hump in the light curve at the beginning

of 1983 is probably due to another burst (a_3) occurring 360 days after a_2, when the previous one had not yet reached the minimum (González–Riestra et al. 1998).

A new minor outburst took place in March 1985 (b_1) and was followed after about 340 days by a second maximum in January 1986 (b_2). These two outbursts might be considered as belonging to the same active phase, in spite of the fact that the star reached the minimum luminosity in between. Indeed, the time interval between the two maxima is nearly the same as that of the previous (1980–83) and the following (1994–97) active phases. After 1986 AG Dra remained in quiescence for 8 years, until the most recent major active phase which started in June 1994. This phase was characterized by four light maxima (at the time of writing this paper), in June 1994 (c_1), June 1995 (c_2), July 1996 (c_3), and June 1997 (c_4) (Montagni & Maesano 1997, Tomov 1996, Mattei 1997, Viotti et al. 1998) separated by nearly the same time interval of about 360 days. In passing we note that another small light maximum is present 330 days before c_1, which is coincident with the maximum no.12 of the 380 days periodicity claimed by Bastian (1998).

Estimates of the visual magnitudes at the time of the IUE observations can also be obtained through the Fine Error Sensor (FES) onboard of IUE. Since AG Dra was frequently observed during the lifetime of IUE, there is a rather good set of photometric points simultaneous with the UV data (Fig. 1). The FES counts have been converted into magnitudes following the expressions given by Pérez & Loomis (1991) for time sensitivity degradation and conversion into magnitudes (no colour correction has been applied). These expressions are applicable to the so-called FES *old reference point*, which was used until January 1990 at GSFC and until July 1990 at VILSPA. The measurements taken with the *new reference point*, have been converted into magnitudes with the expression given by Pérez (1990), again without colour correction. Measurements in the period 1994–1996 were taken at a different position in the FES (the *offset reference point*, used to overcome the problems of scattered light into the telescope), for which no photometric calibration exists. We have used the same calibration as for the "new" reference point, so these magnitudes are inaccurate, and are shown here only as an indication of the relative brightness variations. FES data taken in the period between 1990 and 1994 are not shown in the figure since they are affected by contamination by scattered solar light, which could not be accurately removed for that period. This correction has been made for the measurements of the last 1995 outburst. It should be finally recalled that the FES response curve is much broader than that of the V–band. Therefore the two photometric systems cannot be directly compared.

The recent active phase of AG Dra was monitored, in coordination with the IUE observations, by F. Montagni & M. Maesano in BVRI and by M. Tomova & N. Tomov in UBV. As discussed by Montagni et al. (1996) AG Dra increased its brightness in all the photometric bands, up to the longest wavelength ranges, during the outbursts, which suggests that the variable source substantially contributes also to the emission near 1 μm. Like in quiescence, the amplitude of the variation was the largest in U also during outburst as the result of the presence of a strong and variable Balmer continuum excess.

It is known since the earlier work of Meinunger (1979) that the orbital motion of the AG Dra system is marked during quiescence by the cyclic modulation of the U–band light curve with a period of about 554 days. This periodicity has been later confirmed among others by Kaler (1987) and Skopal (1994). The modulation is also present, but with a smaller amplitude, in the B-band light curves and is barely detectable in V (Meinunger 1979, Skopal & Chochol 1994). The association of the U–band periodicity with the orbital motion of the binary system was definitely confirmed by the radial velocity curve of the K star spectrum, which gives nearly the same period and the appropriate quarter of phase shift between the velocity and the photometric curves (Garcia 1986, Mikolajewska et al. 1995, Smith et al. 1996). However, as will be discussed later, the U–band minima are not associated with eclipses of the hotter component of the system. They could be rather due to occultation of either an extended ionized nebula, or the regions near the K star (in particular its wind) which are ionized by the hot star (see e.g. Proga et al. 1998). In this work we shall adopt the following ephemeris for the U–band photometric maxima: Max(U) = JD2443886 + 554 E (Meinunger 1979). Comparison with Skopal's (1994) ephemeris shows a minimal difference of a few days between the maxima computed for the present days. Recent works have revealed other periodicities in the V band during active phases: 380 days (Bastian 1998) and 350 days (Friedjung et al. 1998, Petrík et al. 1998). This period is most likely associated with the cool giant.

To summarize, there are two main features which characterize the optical light curve of AG Dra: (i) the constant visual magnitude at minimum (besides the modulation by the orbital motion), and (ii) the apparent impredictability of the beginning of the active phases. This suggests that AG Dra is generally in a kind of a nearly permanent *normal state*. This state is occasionally subject to perturbations which give rise to a substantial increase of the optical luminosity (the $outbursts$). The scope of this work is to describe the normal state of AG Dra, on the basis of the multiwavelength observations during quiescence, and to give some possible approaches for an empirical model of the activity phases of AG Dra.

3. Observations

3.1. IUE observations

In this work we have used IUE data as processed through the ESA-INES system. A full description of the system, as well as a discussion of the differences with respect to the NEWSIPS processing system can be found in Rodríguez–Pascual et al. (1999). In short, the INES system performs an improved extraction of the low-resolution spectra from the bi-dimensional SILO files. This extraction overcomes some of the problems found in the NEWSIPS–SWET extraction, such as the handling of weak miscentered spectra, or strong emission lines superimposed on weak continua, which is specially relevant for the type of spectra considered here. The INES system also provides "re-

binned" high resolution spectra, that is, high resolution spectra resampled at the low resolution wavelength bin. These spectra are only resampled and no smoothing or convolution with the low resolution PSF has been performed. Therefore the spectral resolution of these spectra is higher than in low resolution spectra.

In this paper we shall concentrate on the low resolution IUE observations, including also the high resolution rebinned spectra. The detailed analysis of the high resolution data is left for a forthcoming paper. However, when necessary, reference to the high resolution data will be made.

For most of the low resolution observations (especially with the SWP camera), both IUE apertures were used, in order to have in the large aperture the continuum and the weak lines well exposed, and in the small aperture the strongest emission lines (C IV and He II) not saturated. The spectra taken through the Small Aperture have been put into an absolute flux scale by scaling them to the Large Aperture spectrum in non–saturated regions of the continuum taken during the same observing run.

For this investigation we have measured the most prominent emission lines and two continuum fluxes, at 1340 and 2880 Å (20 Å wide bands), which are indicative, as suggested in Paper II, of the continuum of the hot star and of the nebular component, respectively. The measurements are summarized in Fig. 2 and in Table 1, where we also include the FES and Visual magnitudes, the latter interpolated in the AAVSO 10-days means. A full identification of the lines can be found in Paper I. The examination of the high resolution data shows that the contribution of the Si IV doublet to the 1400 Å feature is much smaller than that of the O IV] multiplet. Also, the anomalously large width of this feature on 1995 July 28 reported in Greiner et al. (1997) is due to a grazing cosmic ray affecting the spectrum. All the measurements reported are corrected for interstellar absorption using a colour excess of E_{B-V}=0.06, as derived in Paper I. Examples of IUE spectra of AG Dra are shown in Fig. 3.

3.2. Optical observations

The optical spectrum of AG Dra has been monitored by one of us (TI) at the Asiago Astrophysical Observatory since 1982 with the 1.2 m and 1.82 m telescopes, using a variety of spectrographic equipment. For the present work we have analysed a set of homogeneous spectrophotometric material collected during 1985–86 at the 1.2 m Asiago telescope using the prismatic spectrograph Camera VI, and since 1993 at the Cima Ekar 1.82 m telescope using a Boller & Chivens spectrograph which provides a low resolution spectrum in the blue region (4000–5100 Å). The Cima Ekar spectrograms were calibrated into absolute fluxes using the standard star BD +33° 2642 (Stone 1977). The observed spectral region includes strong emission lines of hydrogen, He II, and He I, and weaker lines of Fe II and N III. During the active phases the strongest emission lines, namely He II λ4686, Hβ and Hγ, present extended wings (FWZI $\sim$ 3000 km s^{-1}) whose intensity is generally 10% that of the emission peak. These wings have been measured separately from the narrow emission peaks using a two–gaussian fit. We recall that

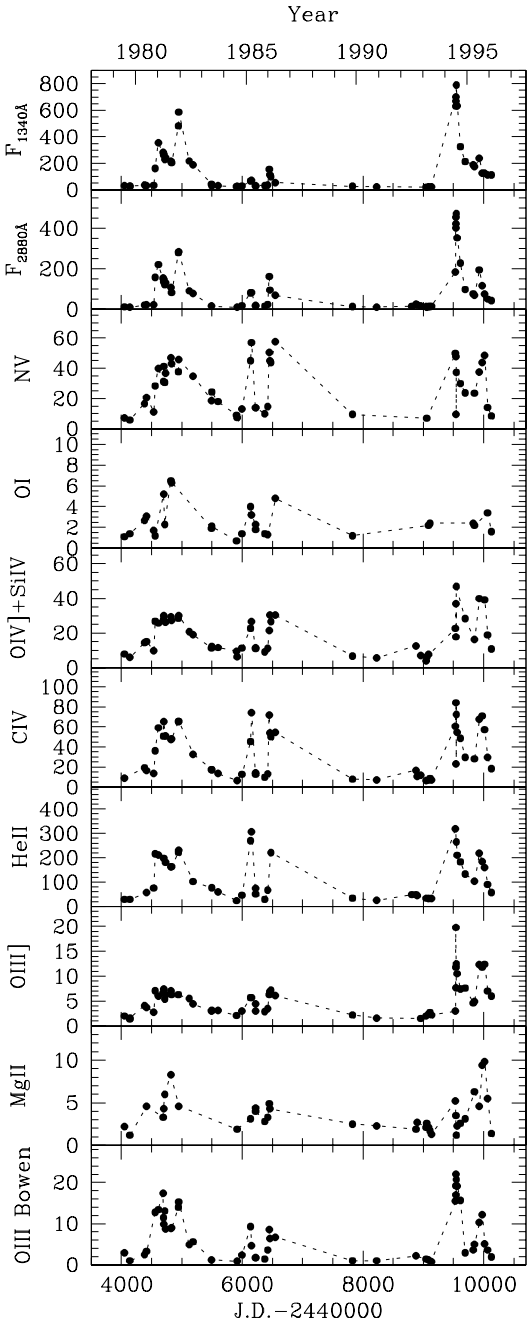

Fig. 2. Examples of IUE light curves for two continuum bands 20 Å wide centered at 1340 and 2880 Å, and several representative emission lines. Units are 10^{-14} erg cm^{-2} s^{-1} Å^{-1} for the continuum fluxes, and 10^{-12} erg cm^{-2} s^{-1} for the line intensities. All measurements have been corrected for an interstellar extinction of E_{B-V}=0.06.

broad wings were observed in the He II 1640 Å emission line during the 1981 bright phase (Viotti et al. 1983). Weak emissions of [O III] λ 4363 (flux $\sim 3\times10^{-13}$ erg cm^{-2} s^{-1}) were detected on the spectra taken in December 1994 and in the following ones. The [O III] λ 5007 line was not detected in any of the spectra.

Table 2 gives the fluxes of the main optical emission lines and, when possible, of the emission wings from October 1985 to

Table 1. Ultraviolet continuum and line fluxes

Date	JD	Phase	V	V_{FES}	Cont 1340	Cont 2880	NV 1240	OI 1340	OIV]+ 1400	NIV] 1486	CIV 1550	HeII 1640	OIII] 1663	HeII 2512	HeII 2733	MgII 2800	OIII 3133	HeII 3200
29 Jun 79	4054	0.303	9.83	9.90	31	12	7.1	1.1	7.9	2.3	9.0	29.2	2.0	1.5:	1.0	2.2	2.9s	1.7:s
25 Sep 79	4142	0.461	9.81	9.88	26	10	5.8	1.4	5.9	1.7	5.9:	29.4s	1.4	0.9	1.4s	1.2s	1.0	1.4
27 Sep 79	4144	0.465	9.80	9.81	28					1.7			1.6					
23 May 80	4383	0.897	9.72	9.85	35	21	16.7s	2.7	14.4s	4.1	19.2s		4.1	1.8	1.7:		2.5	1.3
27 Jun 80	4418	0.959	9.85	9.89	33	22	20.7	3.1	15.1	3.9	16.4	57.0s	3.7	1.4	1.5s	4.6s	3.3	2.0
23 Oct 80	4536	1.173	9.86	9.90	34	23	11.1s	1.7	9.7	2.9	13.6	75.7s	2.8	1.4	2.4			4.3
15 Nov 80	4559	1.214	9.11	9.26	161	158s	28.3s	1.2	26.8	6.7	36.0	216.4s	7.1	6.2s	6.0:s		12.8s	5.3
8 Jan 81	4613	1.312	8.35	8.90	355	221	39.9		25.7	8.2	59.1	211.2s	6.0		5.5		13.4	6.7
28 Mar 81	4692	1.455	8.92	9.22	282	154r				4.8			6.7		4.2r	3.3r	17.4r	
4 Apr 81	4699	1.466	8.94	9.31	267	137r	31.2r		27.8r	10.1r	50.7r			6.0r	3.7r		11.5r	
5 Apr 81	4700	1.469	8.96	9.30	267	147r	41.2s	5.2	30.0	6.5	65.2s	7.7s	7.4	4.3	5.6	4.3s	9.9	7.9
24 Apr 81	4719	1.502	8.97	9.31	230	121r	30.6r	2.3r	26.7r	9.0r	45.3r		5.4r	7.4r	5.2r	6.0r	13.1r	5.2r
10 May 81	4735	1.532	9.01	9.40	243	131	36.6s		26.2s	6.8	50.9s	180.6s	6.2	3.9	0.8		8.7	4.2
3 Aug 81	4820	1.686	9.18	9.47	217s	108	46.9s	6.5s	29.3s	5.3	47.3s	162.8s	7.1	2.9		8.3r	8.9	7.1
14 Aug 81	4831	1.705	9.20	9.47	204	83	43.1s	6.3	27.4	8.2	48.1	164.1s	6.3	3.8	3.6		9.0	
5 Dec 81	4944	1.909	8.38	8.89	482s	280s	37.7s		28.5s		65.4s	222.0s	6.3s				14.0s	
11 Dec 81	4950	1.920	8.40	8.92	586	284r	45.8	0.6:	30.1	6.9	65.6	230.6s	5.5:	7.4r	4.1r	4.6r	15.3r	6.7r
3 Jun 82	5124	2.234	9.06	9.41	217	91			20.7	6.1			5.5	3.1	3.0		4.9	4.9
4 Aug 82	5186	2.347	9.23	9.55	190	78	34.8s		19.0s	3.9	32.7s	102.9s	4.4	1.6	2.6		5.6	3.6
7 Jun 83	5493	2.900	9.72	9.90	43r	16	18.6r	1.9r	11.3r	3.3r	17.5r		3.0r	1.5	1.7		1.2	3.2
13 Jun 83	5499	2.910	9.77	9.83	33		24.3s	2.1	12.2	3.6	17.1	76.5s	3.1					
22 Sep 83	5600	3.094	9.85	9.83	31		18.0	1.7:	11.6	3.8	13.6	60.0s	3.1					
26 Jul 84	5908	3.650	9.87	9.80	25		9.0	0.7	9.5	1.7		24.1	2.1					
2 Aug 84	5915	3.663	9.85	9.88	26	10	7.3		6.2	1.6	6.5		1.7:	0.8	0.9	1.9	0.9	1.7
23 Oct 84	5997	3.811	9.80	9.77	29	18	13.2	1.4	11.3	2.7	12.7	46.4s	3.0	1.0	1.3		2.4	2.4
13 Mar 85	6138	4.064	9.24	9.48	66	82	45.1	4.0r	22.7	5.1	45.4	269.6s	5.7	6.0	6.6s	3.1s	9.3	12.2
30 Mar 85	6155	4.095	9.31	9.40	71	83	57.0s	3.2	26.7	5.9	74.0s	306.3s	5.7	4.1			4.7	12.7
3 Jun 85	6220	4.213	9.66	9.76	27	19	14.0	2.3	11.5	3.4	14.3	74.3s	4.4	1.4	2.1	4.4	1.8	3.3
9 Jun 85	6226	4.222	9.68	9.70	32	17	13.9	1.8	11.0	3.7	12.8	51.2s	3.0	1.3	1.8	4.0	1.7	2.2
4 Nov 85	6374	4.491	9.91	9.84	32	15	9.8	1.4	9.0	2.9:	9.7	29.6r	2.9	1.5	1.4	2.8	1.4	2.9
24 Dec 85	6424	4.580	9.88	9.79	37	24	14.7	1.3	11.1	4.1	13.2	67.0s	3.5	1.7	2.3	3.3	3.6	3.4
18 Jan 86	6449	4.625	9.24	9.23	155	162s	50.5s		21.5	9.1	71.6s	356.3:s	6.3	7.7s	10.1s	4.9s	8.6	15.8
31 Jan 86	6462	4.649	9.26	9.37	114	95	44.9		30.4	7.0	54.1		6.9	5.1	6.9	4.3	6.4	20.6
14 Feb 86	6476	4.675	9.33	9.29	98		43.9		26.7	10.0	50.0	221.7s	7.2					
30 Apr 86	6551	4.810	9.40	9.48	54	69	57.6s	4.8	30.3s	6.7	54.5s		6.1	5.1			6.7	7.9
27 Oct 89	7827	7.113	9.92	9.91	27	13	9.5	1.2s	6.7	1.8	7.9	34.4s	2.2	1.2	1.0	2.5	1.0	1.2
29 Nov 90	8225	7.832	9.93	10.04*	23	11	8.6:		5.6	1.7	7.1	25.6	1.6	0.6	1.0	2.3	1.0	1.8
8 Jul 92	8812	8.891	9.86			15r						49.0r		5.7r	0.8r			7.1r
12 Sep 92	8878	9.010	9.89			26			12.6r	4.8r	18.1r	49.0r		2.3	3.1	1.9	2.2	2.3
2 Oct 92	8898	9.046	9.90			22r					10.8r	44.5r		3.7r	2.0r	2.7r		2.0r
3 Dec 92	8960	9.159	9.91			16r			7.1r	3.5r	11.8r		1.5r					
27 Feb 93	9046	9.314	9.93		20	13	8.9:		4.0		6.6	33.9	2.0	1.2	1.7	2.1	1.4	5.0
11 Mar 93	9058	9.336	9.95			10r	7.0		6.1r	1.7r				1.9r	1.3r	2.6r		7.0r
9 Apr 93	9087	9.388	9.96		22	13	8.3:	2.2	7.6	1.6	6.9	32.3	2.4	0.8	1.3	2.1	1.2	0.7
3 May 93	9111	9.431	9.93		21	14		2.4		2.9	8.5	33.7:	2.7	1.2	1.3	1.7		2.8
26 May 93	9134	9.473	9.92		23	15	6.6:			1.6	7.1	33.3	2.2	1.0	1.4	1.3	0.8	1.2
29 Jun 94	9533	10.192	8.76			185r	49.9r		22.7r	3.9r	60.7r	319.6r	3.0r	8.0r	11.3r	5.2r	15.5r	20.0r
4 Jul 94	9538	10.203	8.56		700s	402s	122.2:s		104.8:s	22.4s			19.8s	5.2s	7.3r	3.5r	19.2s	14.8s
6 Jul 94	9540	10.205	8.51		630	422	47.7		36.9	12.8	84.0	329.1:s	11.8	3.2	5.6s		22.0	4.2
9 Jul 94	9543	10.210	8.38		668r	455r	9.5r		17.8r	4.3r	23.0r		7.7r				17.0	11.6
12 Jul 94	9546	10.217	8.32		789	473	37.3s	2.3:	46.8	11.8	72.3	265.0	12.5	7.5	9.7	1.2s	20.7	9.5
27 Jul 94	9561	10.244	8.38		634	353r	19.2:			8.9	54.4	210.5s	10.5s	4.7r	4.4r	2.3r	19.1	5.8
17 Sep 94	9613	10.338	8.67		326	228	29.9r		24.6:	3.3	48.7	183.4	7.4	7.8	6.5	2.6	15.7	12.4
6 Dec 94	9693	10.481	9.45		214	98	23.8r	2.4:	28.3s	3.1	29.8	133.5s	7.6	2.5	3.6	3.1	2.9	6.8
20 Apr 95	9828	10.726	9.64		189	77		2.4	15.8:	6.1			4.6	2.5	2.7		3.6	2.8
8 May 95	9846	10.757	9.64		175	70	23.5r	2.2r	16.2s	3.3	28.2	103.6s	4.9	2.0	2.4	6.3	5.0	4.3

Table 1. (continued)

Date	JD	Phase	V	V_{FES}	Cont 1340	Cont 2880	NV 1240	OI 1340	OIV]+ 1400	NIV] 1486	CIV 1550	HeII 1640	OIII] 1663	HeII 2512	HeII 2733	MgII 2800	OIII 3133	HeII 3200
28 Jul 95	9927	10.904	8.94		238s	195	37.6r	10.5:	39.9r	14.4	67.6	219.4	12.3	2.9	5.3	4.6	10.3	6.8
14 Sep 95	9975	10.991	9.28		126s	116	43.5r	8.8:	33.9:s	12.8	70.8	184.5s	11.8	4.8	4.8	9.4	12.2	4.4
25 Oct 95	10016	11.065	9.51		125	75	48.5		39.2s	12.8	57.2	160.3s	12.4	2.9	3.7	9.8s	5.1	5.7
12 Dec 95	10064	11.151	9.80		111	51	14.1	3.4	18.9	6.6	29.5	90.3	7.0	3.8	2.4	5.5	3.6	3.8
14 Feb 96	10128	11.266	9.72		113	43	8.5	1.6	10.7	7.8	18.5	57.9	6.0	0.9	2.2	1.4	1.9	2.0

* "new" FES reference point (see text)
J.D. = J.D.-2440000.
s Small Aperture. Scaled to LAP with continuum in non saturated region
r High resolution rebinned spectrum (see text)
: Could be marginally saturated (1-2 pixels in the extracted spectrum)
V interpolated in 10 days means from AAVSO
Phase according to Mikolajewska et al. (1995)
Reddening corrected line intensities in 10^{-12} erg cm^{-2} s^{-1}
Reddening corrected continuum fluxes in 10^{-14} erg cm^{-2} s^{-1} Å^{-1}

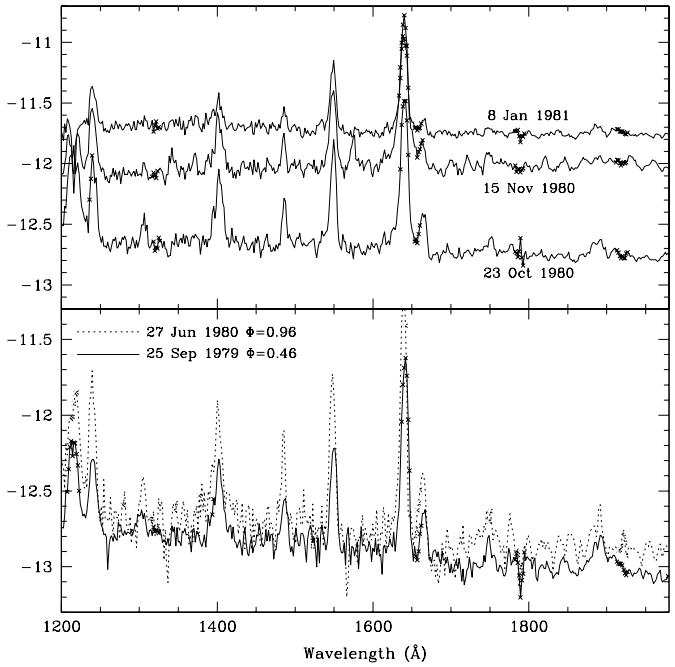

Fig. 3. Examples of spectral variations in the short wavelength region of IUE. *Upper panel:* The early phases of the 1980–81 outburst. *Bottom panel:* Orbital modulation of the spectrum during quiescence. Ordinates are logarithms of dereddened fluxes in erg cm^{-2} s^{-1} Å^{-1}.

May 1986, and from January 1993 to June 1996. All the fluxes were corrected for an interstellar extinction of E_{B-V}=0.06, as discussed above. Fig. 4 shows the variation of the strongest optical emission lines during 1985–86 and 1994–97. We have included in this figure data from Mikolajewska et al. (1995) for the 1985–86 active phase.

3.3. X–ray observations

For the present study we shall make use of the EXOSAT observations of AG Dra during 1985–86, and of the ROSAT observations during 1990–97. EXOSAT pointed AG Dra four times, on 15 March 1985 and 14 February 1986 at the time of the b_1 and b_2 light maxima, and during the minimum phase between them, on 5 June 1985 (Φ=0.22) and 9 November 1985 (Φ=0.50). During the two quiescence pointings of EXOSAT, the count rate with the thin Lexan filter (LE) was high (0.051 ± 0.004, and 0.064 ± 0.004 s^{-1}, respectively) with no evidence of eclipse near phase 0.50. The LE count rate dramatically dropped to 0.0098 ± 0.0010, and to <0.003 s^{-1} (3σ upper limit) at the time of the b_1 and b_2 light maxima, respectively (Viotti et al. 1998).

The ROSAT observations of November–December 1990 (ROSAT Sky Survey with PSPC) and during April 1992 to February 1996 (PSPC and HRI), are described in Greiner et al. (1997). For the present study we shall make use of the HRI data and of a single PSPC observation with the Boron filter, converted into PSPC count rates.

4. Data analysis

4.1. AG Dra in quiescence

The large amplitude of the variations of the U–band light curve during quiescence, which are clearly associated with partial occultations of the sources of hot radiation (hot stellar component of the system and ionized circumstellar nebula), should have its counterpart in the IUE spectra. Indeed the inspection of spectra taken at different orbital phases during quiescence, has shown the presence of marked variations. An example is illustrated in Fig. 3 which shows the variation of the IUE short–wavelength spectrum during quiescence from phase 0.45 (25 September 1979) to 0.96 (27 June 1980).

In order to analyze quantitatively this effect, we have selected 20 short wavelength and 19 long wavelength IUE observations which correspond to minima of the visual luminosity (V $\geq$ 9.7). We have not included in this dataset the two observations taken between the 1985 and 1986 maxima. The data from the different orbital cycles have been folded with the 554 d period, and the resulting curves are shown in Fig. 5. For comparison

Table 2. Optical emission line fluxes

Date	J.D.	H_γ	[OIII] 4363	HeI 4471	HeII 4541	NIII 4640	HeII^n 4686	HeII^b 4686	H^n_β 4861	H^b_β 4861	HeI 5015
25 Oct 1985	6364	3.06		0.21	0.21		6.31		8.48		0.33
21 Jan 1986	6452	12.5	0.21	1.19	1.15	0.29	33.9	2.60	24.3	1.60	2.39
22 May 1986	6573	10.5	0.14	1.08	0.71		15.3		24.1		1.62
10 Jan 1993	8998	3.98		0.41	0.37		6.00		11.4	0.96	0.39
05 Jan 1994	9358	8.16		0.79	0.59		10.0	0.79	22.9	1.62	0.69
01 Jul 1994	9535	11.9		2.90	0.99	0.53	27.0	3.58	31.3	4.25	3.82
26 Dec 1994	9713	7.43	0.21	0.94	0.69	0.23	12.3	1.37	19.2	2.63	1.31
19 Aug 1995	9950	10.52	0.43	1.52	0.68	0.34	15.6	2.42	24.8	4.01	2.31
03 Jan 1996	10086	5.62	0.25	0.79	0.71	0.14	8.67	0.99	16.2	1.23	0.56
06 Jun 1996	10241	6.15	0.32	0.68	0.82		15.3		16.2		0.95

J.D. = J.D.-2440000

Emission line fluxes (in 10^{-12} erg cm^{-2} s^{-1} Å^{-1}) dereddened for E_{B-V}=0.06

^{n} Narrow component (see text)

^{b} Broad component (see text)

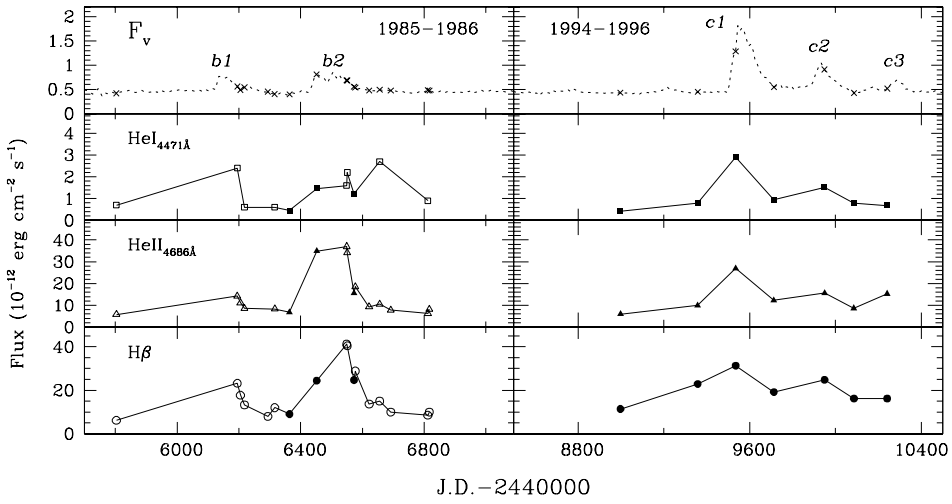

Fig. 4. Variation of the intensity of some of the strongest optical emission lines during the 1985–86 and 1994–96 activity phases. For HeII 4686 Å and Hβ we have plotted only the intensity of the narrow component. Also shown in the figure are data from Mikolajewska et al. (1995) corresponding to the period 1985–86 (open symbols). Line intensities have been corrected for interstellar reddening. The V–band flux curve (from the AAVSO magnitudes) is shown for comparison. Crosses mark the time of the optical spectroscopic observations.

the figure also shows the behaviour of the u Strömgren fluxes published by Kaler (1987), which describe the orbital modulation better than the broader U–band magnitudes. Kaler's data refer to the period from July 1976 to September 1980 (just before the first outburst discussed here), and cover three consecutive cycles. The u–band fluxes near maximum show significant cycle–to–cycle variations within a range of about 30%, while the fluxes at minima are much closer to each others. The light curve presented in Fig. 5 is a smoothed average of the three cycles given by this author.

Shown in the bottom panel of Fig. 5 are the EXOSAT and ROSAT observations taken during quiescence. In both cases the data have been normalized to the corresponding average countrate. In the case of EXOSAT the points shown correspond to June and November 1985, the period between b_1 and b_2 outbursts. The ROSAT fluxes, as discussed by Greiner et al. (1997), were constant during quiescence, except for a slight decrease at phase 0.45.

The overlap of the IUE light curves from different cycles of the orbital motion (Fig. 5) shows a marked phase modulation especially of the higher ionization emission lines. The modulation is very clear in the graph of the N V flux, which near phase zero is twice as large as near phase 0.5, and well matches the u light curve. A similar large amplitude variation is seen in the CIV resonance doublet, the λ1400 blend, and the He II 2711 Å line. The modulation in the stronger He II 1640 Å line is not as evident, most likely due to the uncertainty introduced by the scaling of small aperture measurements. The low ionization MgII doublet appears fairly constant, but for a single observation of 27 June 1980, a few months before the major 1980 outburst (see Table 1). A slight flux decrease is present near phase 0.5. Note however that the measurement of this doublet at low resolution is seriously affected by the strong interstellar lines which could mask the line variability.

The short wavelength continuum appears only slightly modulated along the orbital phase ($\approx$ 30%), much less than the nearby NV line and the continuum flux at 2880 Å.

The light curves in Fig. 5 show a remarkable stability, taking into account that they cover seven orbital cycles. The only large deviation is observed in two points corresponding to 1989–90, which are systematically lower.

Table 3. UV orbital modulations during quiescence

	Orbital Phase			
	All points	0.75–1.25	0.25–0.75	max/min
F(1340 Å)	28.3±1.4 [18]	32.0±1.9 [9]	24.7±1.2 [9]]	1.30±0.14
F(2880 Å)	15.8±1.1 [19]	18.5±1.4 [11]	12.1±0.7 [8]	1.52±0.20
N V	12.9±1.7 [13]	16.5±1.8 [8]	7.2±0.5 [5]	2.28±0.41
O I	1.8±0.2 [13]	2.0±0.2 [8]	1.6±0.3 [5]	1.27±0.41
O IV]+Si IV	9.2±0.8 [18]	10.7±0.9 [11]	6.7±0.7 [7]	1.59±0.30
N IV]	2.6±0.2 [20]	3.2±0.3 [11]	1.9±0.1 [9]	1.72±0.29
C IV	11.3±1.0 [19]	13.7±1.1 [12]	7.2±0.4 [7]	1.90±0.27
He II(1640 Å)	42.3±4.1 [17]	51.8±5.1 [10]	30.8±1.3 [7]	1.68±0.24
O III]	2.5±0.2 [18]	2.9±0.2 [10]	2.0±0.1 [8]	1.42±0.21
He II(2511 Å)	1.7±0.3 [18]	2.1±0.4 [11]	1.1±0.1 [7]	1.87±0.64
He II(2733 Å)	1.4±0.1 [18]	1.6±0.2 [10]	1.2±0.1 [8]	1.37±0.31
Mg II	2.2±0.2 [13]	2.8±0.5 [5]	1.9±0.2 [8]	1.49±0.38
O III Bowen	1.7±0.2 [14]	2.0±0.3 [8]	1.2±0.2 [6]	1.69±0.48
He II(3200 Å)	2.7±0.4 [19]	2.8±0.5 [11]	2.7±0.8 [8]	1.04±0.50
	Orbital Phase			
	0.00–0.25	0.25–0.50	0.50–0.75	0.75–1.00
F(1340 Å)	30.7±2.0 [3]	24.4±1.5 [7]	25.5±0.5 [2]	32.7±2.7 [6]
F(2880 Å)	20.0±2.4 [5]	12.4±0.7 [7]	10.0 [1]	17.2±1.7 [6]
N V	12.9±2.6 [3]	6.6±0.4 [3]	8.1±0.8 [2]	18.7±1.9 [5]
O I	1.5±0.2 [3]	1.8±0.3 [4]	0.7 [1]	2.2±0.3 [5]
O IV]+Si IV	9.5±1.2 [5]	6.3±0.7 [5]	7.8±1.7 [2]	11.7±1.4 [6]
N IV]	3.4±0.5 [5]	1.9±0.2 [7]	1.7±0.1 [2]	3.1±0.4 [6]
C IV	12.4±1.2 [6]	7.3±0.5 [6]	6.5 [1]	15.0±1.8 [6]
He II(1640 Å)	52.7±7.1 [5]	32.0±0.9 [6]	24.1 [1]	50.9±8.2 [5]
O III]	2.7±0.2 [4]	2.0±0.2 [7]	2.1 [1]	3.1±0.3 [6]
He II(2511 Å)	2.2±0.4 [5]	1.2±0.2 [6]	0.8 [1]	2.0±0.8 [6]
He II(2733 Å)	2.0±0.4 [5]	1.2±0.1 [7]	0.9 [1]	1.3±0.2 [5]
Mg II	2.4±0.2 [3]	1.9±0.2 [7]	1.9 [1]	3.4±1.1 [2]
O III Bowen	1.9±0.5 [3]	1.3±0.2 [5]	0.9 [1]	2.1±0.4 [5]
He II(3200 Å)	2.5±0.5 [5]	2.8±0.9 [7]	1.7 [1]	3.0±0.9 [6]

Mean value ± standard deviation [number of points]
Reddening corrected continuum fluxes in 10^{-14} erg cm^{-2} s^{-1} Å^{-1}
Reddening corrected line intensities in 10^{-12} erg cm^{-2} s^{-1}

The small number of points precludes a detailed analysis of the phasing of the emission lines strengths. To overcome this problem, we have tried two different approaches. Firstly, we have averaged the points in two phase intervals: in the ranges 0.25–0.75 and 0.75–0.25, which mark the *minimum* and the *maximum* of the u light curve, respectively. The results are shown in the first part of Table 3, where we also give the average of all the points and the max/min flux ratio. Because of the procedure followed, the max/min ratios should obviously be considered as lower limits to the actual amplitude of the flux variation during the orbital motion. Table 3 shows that the high ionization emission lines have a large flux ratio, definitely larger than that of the long wavelength continuum and much larger than that of the low ionization emission lines and of the short wavelength continuum.

The second approach has been to divide the light curves into smaller bins. Taking into account the limited set of data, we have chosen a binsize of a quarter of cycle, which should enable us to see any asymmetry in the light curves. The mean values are listed in the second part of Table 3. Although the results are hampered by the scarcity of data for the third quarter of phase, there is an indication, also confirmed by an inspection of Fig. 5, that for the most modulated features the flux increase after minimum is steeper than the previous decrease phase.

4.2. AG Dra during outburst

During the IUE lifetime AG Dra underwent three phases of activity, two of which were characterized by two optical maxima, while the last one had at least four maxima, of which only the first two were observed by IUE (Fig. 1). Fig. 6 summarizes the UV behaviour of AG Dra during the three active phases. In this figure we have plotted (except for the case of the UV colour) values *relative to the average quiescence value* to better represent the flux changes in the different outbursts.

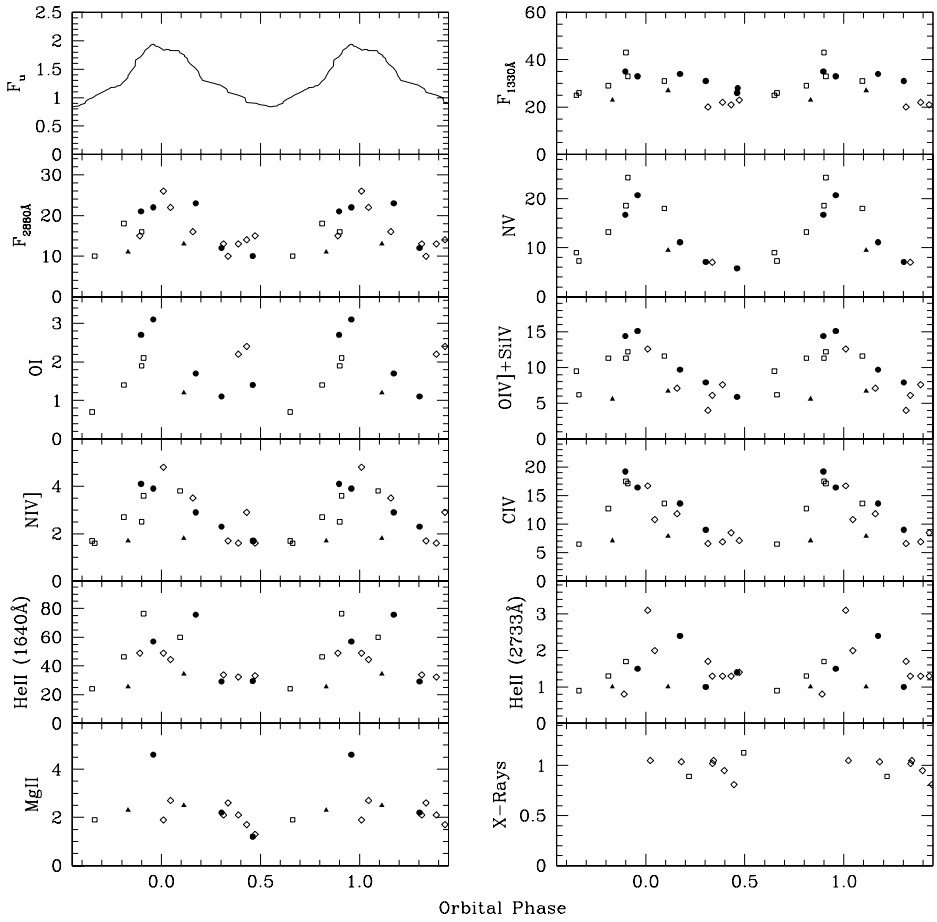

Fig. 5. Orbital variation of UV continuum, UV emission lines and X-rays during quiescence. The light curve in the upper left panel is the smoothed *u* band light curve from Kaler (1987). Continuum fluxes are in 10^{-14} erg cm^{-2} s^{-1} Å^{-1}, and line intensities in 10^{-12} erg cm^{-2} s^{-1}, both dereddened for E_{B-V}=0.06. X–ray points have been normalized to the average countrate during quiescence. The different symbols refer to different epoch as follows: filled circles: 1979–80, open squares: 1983–84, filled triangles: 1989–90, and open diamonds: 1992–93.

The *primary outbursts* were accompanied by a marked increase of UV continuum and line fluxes. In particular, during the two major activity phases (1980–83 and 1994–97) the variation in the UV continuum was much larger than in the optical. On the other hand, in the 1985–86 outburst the increase in the far–UV flux was much smaller, like in the optical, but the emission lines reached intensities comparable to the other active phases. This is also true for the optical emission lines (Fig. 4).

The characteristic two peaks in the visual light curve are largely modified in the UV, and also differ from outburst to outburst. For instance, the second 1981 peak was stronger than the first one in the UV continuum, but of the same amplitude in the He II line. The N V line displays a totally different trend, with a gradual increase and a plateau thereinafter. During the 1985–86 active phase all the fluxes returned to values close to quiescence between the two peaks. This was not the case for the period between the 1994 and 1995 maxima, since the system had not fully returned to quiescence when the second outburst started despite the large separation in time between the first and the second peaks (see also the evolution of the UV colours shown in Fig. 10).

The different evolution of the He II 1640 Å line and of the far UV makes that the ratio of both quantities (to which we shall refer as "equivalent width", although it is not so, strictly speaking), have a dual behaviour. The average value during quiescence is 153±43 Å. It varies during the orbital period between 130 and 170 Å for phases in the range 0.25–0.75 and 0.75–1.25, respectively. During the 1980–81 outburst it decreased to an average of 67±15 Å, with the a_2 outburst having the lower values. The trend was similar in 1994–95, when this quantity decreased to 74±38 Å, although in this case it was lower in the first maximum. The most remarkable difference was in 1985–86, when the effect of the small increase in the far UV continuum and the large increase in the lines acted so that the equivalent width reached values as high as 420 Å in the first peak and 226 Å in the second one. There is only one valid measurement of the helium line for this second peak, but the upper limits derived from the saturated lines indicate that values as high as 500 Å could have been reached.

The behaviour of the C IV, N V and Si IV lines during the first stages of the 1994 outburst deserves special attention. On July 9 the line intensities show a pronounced decrease. This is due to the appearance of strong P Cygni profiles (Fig. 7). These profiles were not present in spectra taken on July 6th. High resolution data of July 12th, although of lower signal–to–noise ratio, does not show the presence of these absorptions either. Similar profiles had already been observed in AG Dra in 1980–81, but only in the N V line (Paper I, Kafatos et al. 1993), and in any case with a small velocity (170 km s^{-1}), while in July 1994 the terminal velocity of the N V doublet can be estimated from Fig. 7 as at least 700 km s^{-1}.

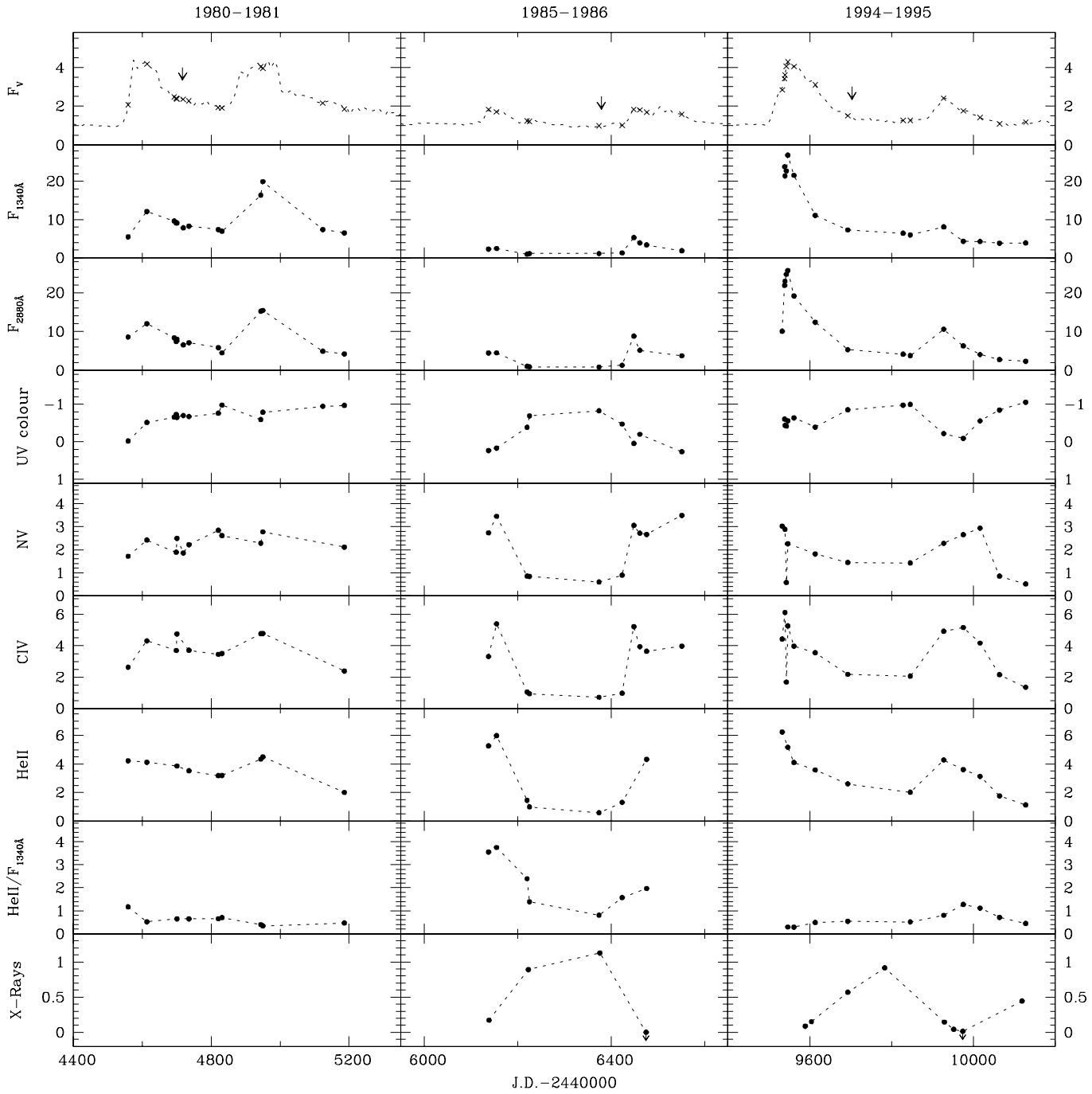

Fig. 6. Detailed IUE light curves of the different outbursts. All fluxes are normalized to the mean value during quiescence out of eclipse, as given in Table 3. The UV colour is defined as –2.5 log(F_{1340}/F_{2880}). The upper panels give the visual fluxes (from the AAVSO light curve), where the crosses mark the times of the IUE observations and the times of orbital phase 0.5 are marked by arrows. The bottom panels show the X–rays light curves from EXOSAT and ROSAT, normalized to the average quiescence countrate, as discussed in the text. Note the minima of the C IV and N V flux on 9 July 1994 (JD 9542) due to the strong P Cygni absorption shown by these lines.

The variations of the X–ray flux during the active periods are also shown in Fig. 6. There is a clear anticorrelation with the visual flux, i.e. low X–ray flux when the visual flux is high (see also the bottom panel in Fig. 9).

Fig. 8 shows the evolution of some of the optical lines during outburst. The equivalent widths of He II 4686 Å and Hβ and the ratio He II 4686/Hβ prior to July 1985 have been taken from Iijima et al. (1987). Data from Mikolajewska et al. (1995) for the 1985–86 period have been used also. The ratio He II 4686/Hβ does not vary substantially during the optical peaks except during b_2, being its average value 0.8$\pm$0.2. The ratio He II/He I also reached high values in the b_2 outburst. In the lower panels of

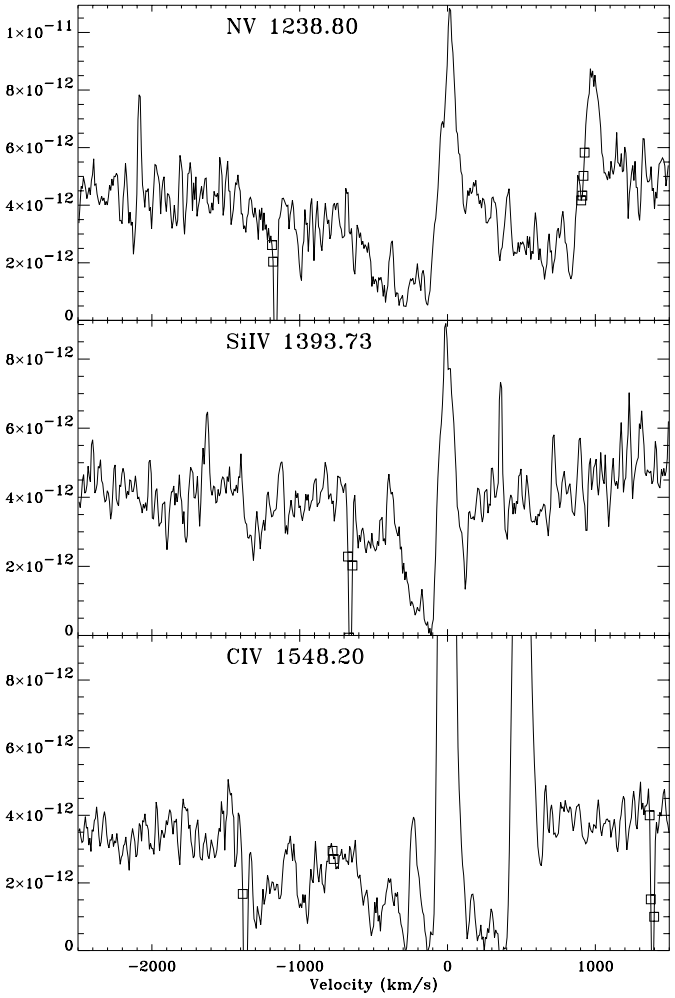

Fig. 7. P Cygni profiles of the UV resonance lines in the high resolution spectrum taken on July 9 1994. Squares mark bad–quality pixels.

this figure we compare the equivalent widths of Hβ and the He II lines at 4686 Å and 1640 Å. There is an indication of slightly smaller equivalent widths of the He II lines at a_2, and a large increase at b_1. The behaviour in 1994–95 was more erratic.

We have plotted in Fig. 9 the intensity of the main UV and optical lines against the visual flux which, as discussed above, has been taken as the parameter describing the level of activity. We have plotted separately the three active phases and for each of them, the two peaks with different symbols, so as to highlight any possible similarity or difference among them. In general, UV continuum and emission line fluxes increase linearly with the optical flux until a given value from which the lines reach a kind of "saturation plateau".

5. Discussion

5.1. Quiescence

IUE observations of AG Dra during quiescence have shown that both the UV continuum and the emission lines (with the possible exception of Mg II) vary in phase with the U–band light curve, with small cycle–to–cycle variations.

The variation of the optical continuum during quiescence was discussed by Kaler (1987). This author confirmed the modulation of the flux already discovered by Meinunger (1979) and showed how the amplitude of the modulation decreases at longer wavelengths (from the u band to 8200 Å). We confirm here the existence of such modulations also in the UV continuum, but with the opposite trend, i.e. smaller modulation at shorter wavelengths. Already at 2880 Å the size of the variation (1.52, as defined in Table 3) is smaller than in the u band (2.35$\pm$0.34, using the same definition). This support the interpretation that the Balmer continuum is the dominant contributor at 2880 Å in quiescence. Current model fits (Mikolajewska et al. 1995, Greiner et al. 1997) show that, during quiescence the flux at 1340 Å is dominated by the longwave tail of white dwarf continuum. The flux in this band varies only by a 30% along the orbital period. This clearly indicates that the white dwarf itself is not eclipsed, in agreement with what was found by Greiner et al. (1997) from the lack of eclipses in X–rays. These authors set an upper limit to the inclination of the system of 85°.

The flux modulation near minimum must be attributed to either occultation, or to the anisotropy of the UV emission, or to a combination of both. Anisotropic emission could occur in the case that regions near the K star are ionized by the WD radiation. Moreover, the occulter cannot be the K star only, but must also include its atmospheric envelope and wind, which might be very extended even if the star is inside its Roche lobe.

As for the emission lines, it seems that the variation of the resonance lines (e.g. N V, C IV) is larger than that of the intercombination lines (e.g. O III]), indicating that they are formed in different regions. Some of the lines (N V, C IV) have light curves which are slightly asymmetric with the rise steeper than the decay and the maximum slightly shifted to earlier phases. The nearly constancy of the flux of the Mg II blend is difficult to understand, unless, as discussed above, the strong interstellar lines on the long wavelength side of the emission is largely affecting the line flux. The Mg II in AG Dra is much stronger with respect to the flux generally observed in single K giant and supergiant stars.

Fig. 5 also suggests some degree of cycle–to–cycle variability. This is not unexpected since also the U and u light curves described earlier by Meinunger (1979) and Kaler (1987), are far from being stable. A smaller amplitude variability on time scale shorter than the orbital period could also be present. A straightforward interpretation is that this is due to variation of the matter flowing from the cool star, as suggested by Friedjung et al. (1998).

The Zanstra temperature can be estimated from the ratio He II/F(1340 Å). Table 4 gives the average Zanstra temperatures as well as the radii and luminosities derived from it (assuming that the WD radiates as a blackbody) for the three quiescence phases, using only data taken between orbital phases 0.75–0.25. During quiescence the average value of the Zanstra temperature is 109600$\pm$5400°K. Assuming that all the observed flux at 1340 Å is due to a blackbody radiating at the Zanstra temperature, and for a distance of 2.5 kpc, we estimate a WD radius of 0.08 $R_\odot$ and a luminosity of 930 $L_\odot$. This can be compared

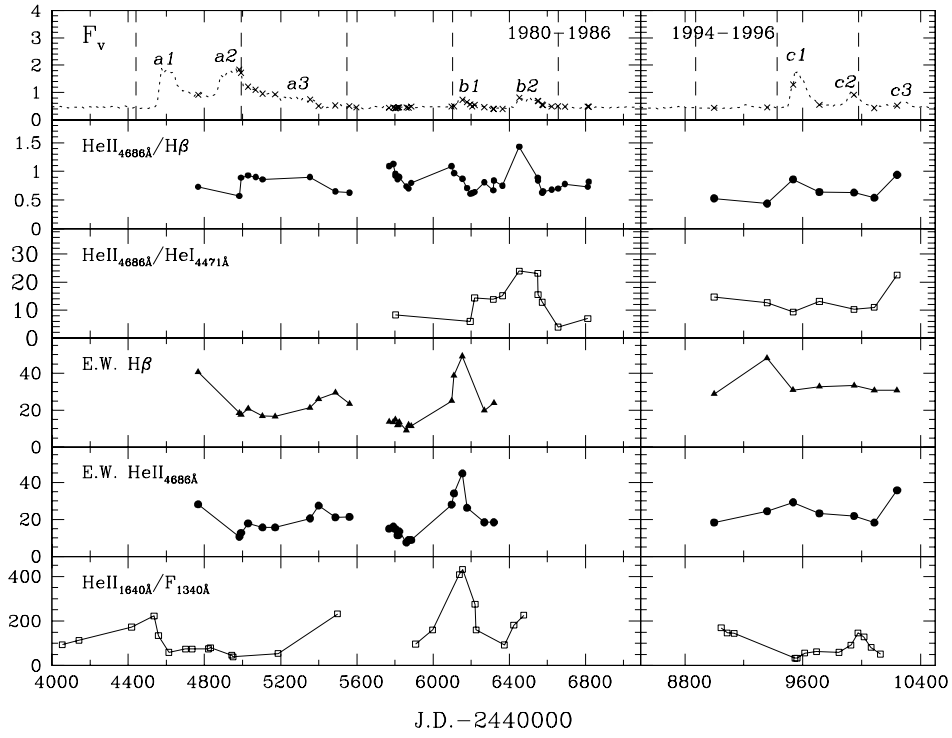

Fig. 8. Variation of ratios of optical lines and equivalent widths during the active phases. Equivalent widths are given in Angstroms. The upper panel shows the V flux light curve for comparison, with the times of the optical spectroscopic observations marked on it as crosses. The dashed lines mark the times of orbital phase 0.

with the results obtained from the EXOSAT and ROSAT observations. Piro et al. (1985) derived a blackbody temperature of 200000°K from the June 1985 EXOSAT observations, in the period of quiescence between the b_1 and b_2 outbursts. Greiner et al. (1997) obtained T=160000±20000°K, R=0.06$R_\odot$, and L=2500 $L_\odot$from a blackbody fit to ROSAT quiescence data. We note that though blackbody and white dwarf atmosphere model fits result in similar best–fit temperatures, a direct comparison between near–simultaneous X–rays (both ROSAT and EXOSAT) and IUE measurements shows that the X–rays temperature is systematically higher than the Zanstra temperature derived from the IUE spectra. Blackbody fits to the ROSAT data typically overestimate the luminosity with respect to WD model atmospheres. It is also true that the use of a "classical" Zanstra method, as we have done, also underestimates the temperature, but for the range of values considered here the difference is only a few thousand degrees (Mürset et al. 1991).

5.2. The active phases

The most relevant difference in the six outbursts observed in the UV is the different behaviour of the continuum and the emission lines. While line intensities reach similar values in all the active phase, the increase in the UV continuum was much smaller in the 1985–86 maxima (only a factor 5 at the b_2 peak, while in the other the flux increased by factors of up to 25, see Fig. 6). This results in a large increase in the equivalent widths of the UV emission lines in that period. Particularly relevant is the behaviour of the equivalent width of the He II 1640 Å line, as discussed below.

The two upper panels of Fig. 10 show colour-colour diagrams computed using the two UV continuum fluxes and the V-band fluxes derived from the AAVSO magnitudes. In both diagrams quiescence and outburst points are clearly separated. We note that the four open squares which appear in the region close to the quiescence points correspond to observations performed between the 1985 and 1986 outbursts, indicating that the system returned to its normal quiescence status between both maxima. From this figure we conclude that the energy distributions are very different in quiescence and in outburst.

The (1340–2880) colour does not show any significant variation in outburst with respect to the quiescence values, except for the 1985–86 maxima and the beginning of the 1995 outburst, where the UV energy distribution appears "redder". Since the major contribution to the flux in the 2880 Å band comes from the recombination continuum, we conclude that there was a large increase in this continuum at the beginning of these outbursts, contrary to what happened in 1980–81 and in 1994. The separation between quiescence and outburst is much more marked in the (1340-V) vs. (2880-V) colour-colour diagram (middle panel of Fig. 10). In fact, both colours were about 1.5 mag. brighter at the outburst maximum. The only exception is again represented by the 1985–86 (1340-V) colours which are systematically "redder" by approximately 1 magnitude, in agreement with the peculiar behaviour of these "hot" bursts as noted above. As for the (2880-V) colour, it is larger (i.e. "redder") in quiescence by about 1.5 magnitudes. In this case the 1985–86 outburst does not show any significative difference.

The bottom panel of this figure represents the logarithm of the equivalent width of the He II 1640 Å line (normalized to the quiescence value) vs. the (2880-V) colour. We have included

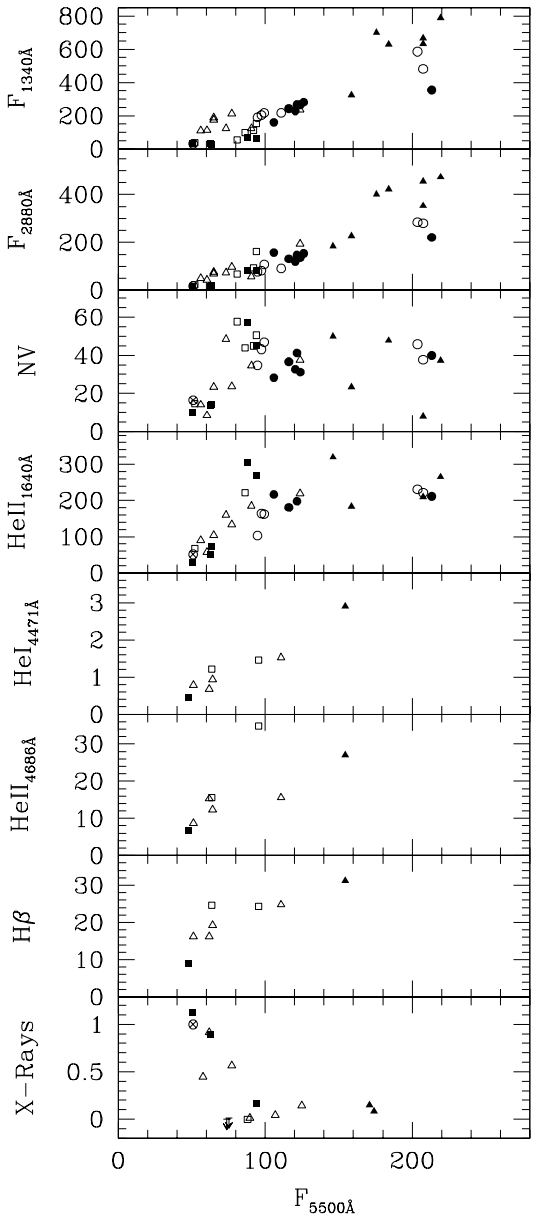

Fig. 9. Continuum and line fluxes and X–rays flux as a function of the V flux during the three activity phases. The different symbols indicate: *circles*: 1980–83, *squares*: 1985–86, *triangles*: 1994–96. For each outburst filled and open symbols represent the first and the second peak, respectively. The crossed circle in each panel represents the average quiescence value (taken as V=9.9 in the visual, and other values from Table 3 near phase 0).

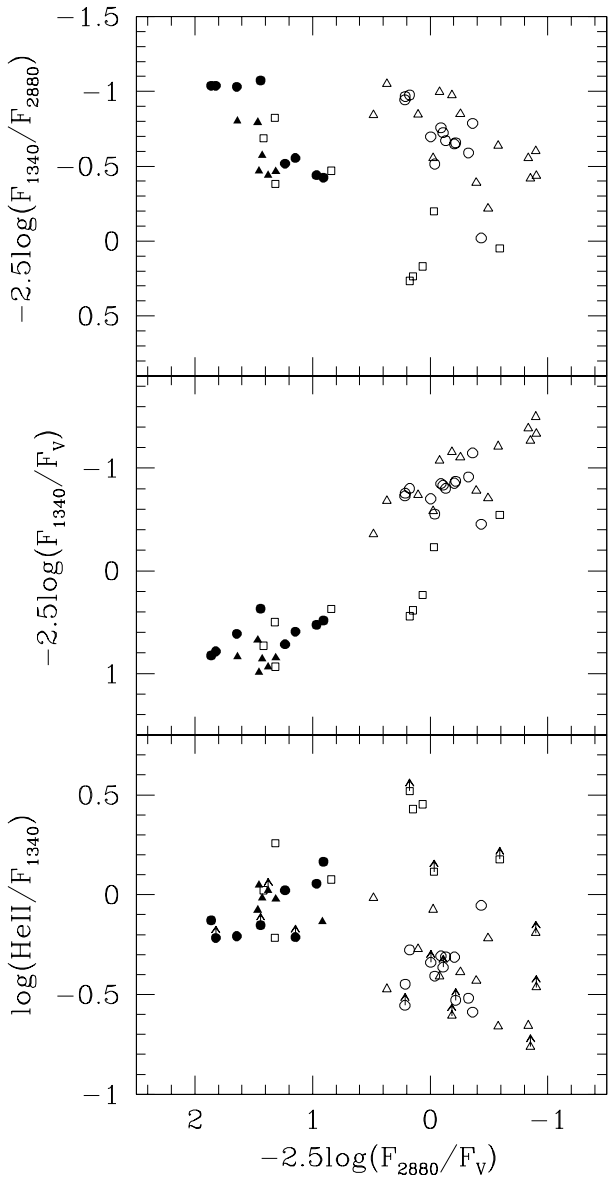

Fig. 10. UV Colour-colour diagrams for the different activity phases of AG Dra. The ratio He II/F_{1340} has been normalized to its average quiescence value. Circles correspond to data prior to November 1984, squares to data taken between March 1985 and April 1986, and triangles to data after October 1989. In all cases filled symbols represent quiescence periods and open symbols active phases. The open squares which appear in all panels close to the quiescence data correspond to observations taken between the b_1 and b_2 maxima.

here some lower limits corresponding to saturated lines not included in previous figures. The larger equivalent widths correspond to the 1985–86 outbursts. Unfortunately there are only lower limits for the beginning of the 1994 outburst, therefore we cannot rule out that the He II line reached high intensities in that epoch, while this possibility seems to be excluded for the 1980–81 maxima.

If we use, as we did for quiescence, the *pseudo* equivalent width of the He II 1640 Å line to derive the Zanstra temperature, we find that during the 1980–81 outburst the temperature decreased from the quiescence value of 112000°K to 94900°K in the a_1 maximum, and to 86000°K in a_2. In 1994–95 the temperature reached minimum values of 83900°K in c_1 and 96400°K in c_2 (see Table 4, where we give for the active periods the range of derived temperatures, radii and luminosities). The corresponding maximum radii were 0.33 (a_1), 0.45 (a_2), 0.53 (c_1) and 0.25 (c_2) $R_\odot$, and the luminosities reached values of 7100 (a_1), 10200 (a_2), 13000 (c_1) and 5600 (c_2) $L_\odot$. On the contrary, the large increase in the equivalent widths in 1985–86 indicates

Table 4. Basic characteristics of the hot component

Event	N. of points	$T_{Zanstra}$	R ($R_\odot$)	L ($L_\odot$)
q1	2	112600±3800	0.09	1100±100
a1	6	94900–105000	0.20–0.33	4400–7100
a2	3	86000–90300	0.25–0.45	3700–10200
q2	3	112200±3900	0.09	1000±100
b1	2	130000–131000	0.11	3100–3400
b12	4	109400±8900	0.09±0.01	1000±200
b2	1	115600	0.14	3400
q3	2	102800±1700	0.08	700±100
c1	5	83900–92300	0.23–0.53	3500–13000
c2	5	96400–106600	0.17–0.25	2100–5600
Quiescence	7	109600±5400	0.08±0.01	900±200

All values computed for a distance of 2.5 kpc
q1: quiescence prior to a_1
q2: quiescence between a_2 and b_1
q3: quiescence between b_2 and c_1
b12: points taken between the b_1 and b_2 outbursts
Quiescence: Average of all quiescence values for orbital phases between 0.75 and 1.25

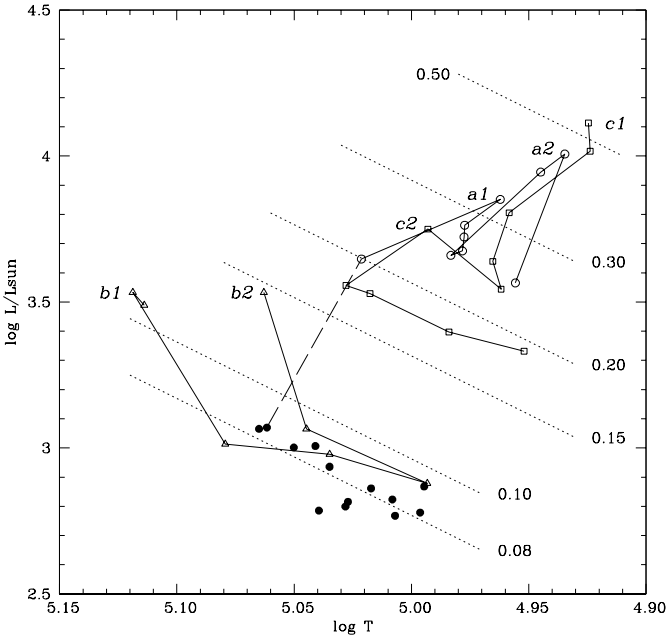

Fig. 11. Evolution of the hot component of AG Dra in the HR diagram. Filled circles are quiescence data. Open symbols refer to active phases, circles: 1980–1982; triangles: 1985–1986, squares: 1994–1996. The dashed line joins the data corresponding to October 23 and November 15, 1980. The dotted lines are lines of constant white dwarf radius, as labeled. The temperature represented is the Zanstra temperature, derived from the He II lines. The luminosities and radius have been computed for a distance of 2.5 kpc, assuming that the hot star radiates as a blackbody.

an increase in temperature: 131000°K in b_1 and 116000°K in b_2 (but values as high as 135000°K could have reached during this second peak, as indicated by the lower limits to the HeII equivalent width derived from saturated lines). Between both maxima the temperature decreased down to 109400°K, close to the average quiescence value. The maximum radius and luminosity for b_1 are 0.11 $R_\odot$ and 3400 $L_\odot$. Similar values were reached in b_2, 0.14 $R_\odot$ and 3400 $L_\odot$, indicating in both cases a large luminosity increase with only a moderate WD expansion.

In this way we can divide the outbursts into "cool" (a_1,a_2,c_1,c_2), and "hot" (b_1, b_2). Greiner et al. (1997) already pointed out that the decrease of the ROSAT fluxes during the 1994–95 activity phases could be understood in terms of a cooling of the expanding white dwarf. The observed decreases in temperature during the "cool" outbursts correspond to increases in the radius of the white dwarf by factors of 2 to 6. This expansion and cooling cause a shift of the energy distribution outside the soft X–rays range. Since a similar decrease of the X–ray flux was observed with EXOSAT at the time of the "hot" b_1 and b_2 outbursts, without a decrease of the Zanstra temperature, we are forced to assume, at least in this case, that the spectrum strongly deviates from a blackbody, due to the combined effect of the presence of an extended atmosphere and an opaque hot wind. These would cause a large increase of the opacity shortward the N^{+4} ionization limit (see for instance the case of SMC 3 discussed by Jordan et al. 1995).

In Fig. 11 we plot the evolution of AG Dra in a (log T, log L) diagram. It is evident from this figure that the evolution from quiescence to the 1985–1986 outburst was very different from that of other active phases.

In the visual the general trend is that weak outbursts are shorter. While the a_2 outbursts started before the a_1 active phase has finished, the system returned to quiescence in the period between b_1 and b_2. The UV follows a similar behaviour (the weak b_1 and b_2 peaks are short), but the situation is more complex, may be in part due to the poorer sampling. For instance, the a_1 maximum was weaker than a_2, but its duration was similar or even longer. The 1994 maximum had a longer "decay time", so that the UV continuum flux was substantially higher than the quiescence value in between the two maxima. As for the emission lines, some of them (N V, O IV], C IV, He II, O III]) kept a nearly constant intensity in the interval between a_1 and a_2, while all returned to quiescence values between b_1 and b_2. Also, the lines had not totally reached the normal values after the 1994 peak, when the second outburst started. A peculiar behaviour is observed at the latest stages of the b_2 outburst (April 30 1986), where the intensity of some of the lines (N V, C IV, He II) increases, while the continuum, both optical and UV, is already in the way down to quiescence values. Although the He II is saturated, a lower limit to its intensity allows us to estimate a Zanstra temperature higher than 135000°K. There is also a difference in the orbital phase at which "cool" and "hot" outburst occur: the 1980–1981 and 1994–1995 peaks took place approximately at phases 0.20 (a_1,c_1) and 0.90 (b_2,c_2), while the minor 1985–1986 peaks took place at phases 0.06 (b_1) and 0.62 (b_2).

In general it seems that, at least for the 1980–83 and 1994–96 events, the first outburst is the most powerful one, and is well marking the beginning of a new activity phase of AG Dra.

We finally note that during the active phases, emission line and continuum fluxes were not affected by eclipses since no evident minima are seen near phase 0.5 in either of the three periods (Fig. 6).

6. Conclusions

The multifrequency study of AG Dra during quiescence and activity has provided a wealth of information which is fundamental for understanding its nature. It is outside the scope of the present work to perform a full interpretation of the data, for which it would be necessary to better know some of the fundamental parameters of the system (distance, separation, radius and luminosity of the cool star). Here we were mostly concerned on the general behaviour during quiescence and outburst. We summarize our main results as follows:

- During quiescence the flux of the higher ionization emission lines and of the near–UV continuum is modulated according to the 554 days orbital motion, suggesting emission from a region placed in the line connecting the two stars and closer to the white dwarf. This region should be extended because of the broadness of the minimum. A contribution to these variation of the heated side of the K-giant facing the WD cannot be excluded, and would not be in contradiction with the relative phasing of the radial velocity and u–band light curves (the WD is in front of the giant at the time of the U maximum, Mikolajewska et al. 1995). However, one of us (TI) has not detected any significant change of the optical photospheric lines along the orbit during quiescence.
- The far–UV flux shows little modulation. The absence of eclipses in this range is suggestive of a not large orbital inclination, in agreement with the non existence of eclipses in X–rays. This result also agrees with a model of X–rays formed on or close to the WD surface.
- The orbit–to–orbit variation of the UV fluxes, in contrast to the stability of the X–ray flux during quiescence, could be related to irregular fluctuation of the density of the cool star wind.
- During the different outbursts AG Dra displayed a variety of behaviours, which cannot be fully described due to the scarcity of observations during the early stages of the outbursts. We can make a gross subdivision of the bursts into cooler (a_1, a_2, c_1, c_2) and hotter bursts (b_1, b_2), depending on whether the He II Zanstra temperature is smaller or larger than in quiescence. It must be noted that the "hot" bursts were much weaker in the UV and optical continuum than the "cool" ones.
- The decay time of the weak "hot" 1985–86 outbursts was substantially shorter than in the other active phases. While the system had not fully returned to quiescence when the a_2 and c_2 outbursts started (approximately one year after the a_1 and c_1 peaks), quiescence levels where reached only 70 days after the b_1 maximum.
- The beginning of the 1994 outburst was marked by the appearance of strong P Cygni absorptions in the high ionization resonance lines, with terminal velocities up to 700 km s^{-1}, never observed before in this object.
  These features might significantly affect the emission line flux observed at low resolution during a critical phase of AG Dra, and lead to wrong interpretations.
- The strong anticorrelation between optical/UV and X–rays during the "cool" outbursts is due to the expansion and consequent cooling of the white dwarf. The temperature of the white dwarf decreases by 10–25%, while its radius expands by factors between 2 and 6, thus causing the observed large brightening of AG Dra. The smaller amplitude "hot" outbursts are due to an increase of the stellar temperature. The onset of an extended atmosphere and of an opaque hot wind would produce a high energy cutoff which would drastically reduce the soft–X ray flux in the EXOSAT sensitivity range, as observed.

Acknowledgements. We would like to thank the efforts of the VILSPA and GSFC IUE staffs, that have provided the scientific community with a precious database, for this and for a great deal of many other astrophysical objects, which will have a fundamental impact in any study in the coming years. R.V. is grateful to Dr. Willem Wamsteker for hospitality at the IUE Observatory of ESA at Villafranca del Castillo (VILSPA). J.G. is supported by the German Bundesministerium für Bildung, Wissenschaft, Forschung und Technologie (BMBF/DLR) under contract No. FKZ 50 QQ 9602 3. R.V. was partially supported by the Italian Space Agency under contract ASI 94-RS-59. In this research we have used, and acknowledge with thanks, data from the AAVSO International Database, based on observations submitted to the AAVSO by variable star observers worldwide. Thanks are also due to R. Luthardt, F. Montagni, M. Maesano, N. Tomov and M. Tomova for informing us about the visual behaviour of AG Dra during the last active phase, and for providing us with their photometric observations. We are grateful to M. Friedjung for stimulating discussions and comments which have greatly improved this paper.

References

Anderson C.M., Cassinelli J.P., Sanders W.T., 1981, ApJ 247, L127
Bastian U., 1998, A&A 329, L61
Friedjung M., Hric L., Petrík K., Gális R., 1998, A&A 335, 545
Garcia M.R., 1986, AJ 91, 1400
González–Riestra R., Viotti R., Greiner J., 1998, In: Wamsteker W., et al. (eds.) Ultraviolet Astrophysics beyond the IUE Final Archive. ESA-SP 413, p. 343
Greiner J., 1996, In: Greiner J. (ed.) Supersoft X-ray Sources. Lecture Notes in Physics, Springer, p. 299
Greiner J., Bickert K., Luthard R., et al., 1997, A&A 322, 576
Iijima T., Vittone A., Chochol D., 1987, A&A 178, 203
Jordan S., Schmutz W., Wolf B., Werner K., Mürset U., 1995, A&A 312, 897
Kafatos M., Meyer S.R., Martin I., 1993, ApJS 84, 201
Kaler J.B., 1987, AJ 94, 437
Lutz J.H., Lutz T.E., Dull J.D., Kolb D.D., 1987, AJ 94, 463
Mattei J.A., 1997, private communication
Meinunger L., 1979, IBVS No.1611
Mikolajewska J., Kenyon S.J., Mikolajewski M., Garcia M.R., Polidan R.S., 1995, AJ 109, 1289
Montagni F., Maesano M., Viotti R., et al., 1996, IBVS No.4336
Montagni F., Maesano M., 1997, private communication

Mürset U., Nussbaumer H., Schmid H.M., Vogel M., 1991, A&A 248, 458
Pérez M., 1990, Record of the IUE Three Agency Meeting, November 1990
Pérez M., Loomis C., 1991, Record of the IUE Three Agency Meeting, November 1991
Petrík K., Hric L., Gális R., Friedjung M., Dobrotka A., 1998, IBVS 4588, 1
Piro L., Cassatella A., Spinoglio L., Viotti R., Altamore A., 1985, IAU Circ. 4082
Proga D., Kenyon S.J., Raymond J.C., 1998, ApJ 501, 339
Robinson L., 1969, Perem. Sviosdi 16, 587
Rodríguez-Pascual P.M., González-Riestra R., Schartel N., Wamsteker W., 1999, submited to A&A
Skopal A., 1994, IBVS No.4096
Skopal A., Chochol D., 1994, IBVS No.4080
Smith V.V., Cunha K., Jorissen A., Boffin H.M.J., 1996, A&A 315, 179
Stone R.P.S., 1977, ApJ 218, 767
Tomov N., 1996, private communication
Torbett M.V., Campbell B., 1987, ApJ 318, L29
Viotti R., 1993, In: Hack M., la Dous C. (eds.) Cataclysmic Variables and Related Objects. NASA Monograph Series, Chap. 11 and 13
Viotti R., Ricciardi O., Ponz D., et al., 1983, A&A 119, 285 (Paper I)
Viotti R., Altamore A., Baratta G.B., Cassatella A., Friedjung M., 1984, ApJ 283, 226 (Paper II).
Viotti R., Giommi P., Friedjung M., Altamore A., 1995, In: Bianchini A., Della Valle M., Orio M. (eds.) Cataclysmic Variables. ASSL 205, 195
Viotti R., González-Riestra R., Montagni F., et al., 1996, In: Greiner J. (ed.) Supersoft X-ray Sources. Lecture Notes in Physics, Springer, p. 259
Viotti R., Badiali M., Cardini D., Emanuele A., Iijima T., 1997, ESA SP-402, 405
Viotti R., Greiner J., González-Riestra R., 1998, Nuclear Physics B (Proc. Suppl.) 69/1–3, 40